OLD DOMINION UNIVERSITY RESEARCH FOUNDATION

DEPARTMENT OF MECHANICAL ENGINEERING AND MECHANICS
SCHOOL OF ENGINEERING
OLD DOMINION UNIVERSITY
NORFOLK, VIRGINIA

ON HIGHER EIGENSTATES OF GOERTLER INSTABILITY IN COMPRESSIBLE FLOW

By

G. L. Goglia, Principal Investigator

and

Alok K. Verma

Final Report (Summer Project)
For the period ending August 31, 1982

Prepared for the
National Aeronautics and Space Administration
Langley Research Center
Hampton, Virginia

Under
Research Grant NAG1-228
W.D. Harvey, Technical Monitor

September 1982

DEPARTMENT OF MECHANICAL ENGINEERING AND MECHANICS
SCHOOL OF ENGINEERING
OLD DOMINION UNIVERSITY
NORFOLK, VIRGINIA

ON HIGHER EIGENSTATES OF GOERTLER INSTABILITY IN COMPRESSIBLE FLOW

By

G. L. Goglia, Principal Investigator

and

Alok K. Verma

Final Report (Summer Project)
For the period ending August 31, 1982

Prepared for the
National Aeronautics and Space Administration
Langley Research Center
Hampton, Virginia 23665

Under
Research Grant NAG1-228
W.D. Harvey, Technical Monitor

Submitted by the
Old Dominion University Research Foundation
P.O. Box 6369
Norfolk, Virginia 23508-0369

September 1982

ON HIGHER EIGENSTATES OF GOERTLER INSTABILITY IN COMPRESSIBLE FLOW

By

Gennaro L. Goglia[1] and Alok K. Verma[2]

1. INTRODUCTION

Instability of viscous flow along a concave surface is in the form of counterrotating streamwise vortices commonly known as Goertler vortices. These three-dimensional vortices have been found to cause transition, indirectly, by interacting with other types of disturbances usually present in the flow. First, theoretical analysis of the problem was done by Goertler (ref. 1). A detailed survey of theoretical and experimental work done in this field was presented by El-Hady and Verma (ref. 2). However, little work has been done on the higher eigenstates of Goertler vortices. D'Arcy was the first to realize the presence of a second mode although his work was not published (ref. 3). Other efforts in this area include work by Aihara (ref. 4), and that of Herbert (ref. 5). Herbert presented the neutral stability analysis of higher modes for an incompressible fluid, and came to the conclusion that the "most dangerous" wavelength of different modes are nearly the same. The same conclusion is arrived at in the present work for compressible viscous fluids. Aihara and Sonoda (ref. 6) discussed the effect of pressure gradient on secondary instability of Goertler vortices.

Experimentally, the presence of secondary instability of Goertler vortices was observed by Wortmann (ref. 7), Bippes (ref. 8), and Aihara (ref. 9). Wortmann observed that secondary instabilities lead to distortion of the interface between two vortices and their oscillation in the spanwise direction.

---

[1] Eminent Professor/Chairman, Department of Mechanical Engineering and Mechanics, Old Dominion University, Norfolk, Virginia 23508.

[2] Research Associate, Department of Mechanical Engineering and Mechanics, Old Dominion University, Norfolk, Virginia 23508.

The purpose of the present work is to investigate the effect of secondary instabilities of Goertler vortices with respect to their growth and amplifications. Another aim of this work is to look into the effects of suction on higher modes of Goertler vortices.

2. PROBLEM FORMULATION AND NUMERICAL PROCEDURE

A comprehensive linear theory of the stability of compressible boundary layers over a curved wall was presented by El-Hady and Verma (refs. 2, 10 and 11). A detailed formulation of the problem, and derivation of governing equations based on orthogonal curvilinear coordinates, is presented in reference 2. The governing equations of the problem are Navier Stokes equations, continuity, energy and equations of state. (See ref. 2, equations 9 thru 13). After appropriate nondimensionalization and linearization, the six eight order system of equations are written as eight first order equations, as follows:

$$(z_m)_y - \sum_{n=1}^{8} a_{mn} Z_n = 0 \qquad m = 1,2...8 \tag{1}$$

$$z_1 = z_3 = z_5 = z_7 = 0 \qquad \text{at } y = 0, \text{ for isothermal wall} \tag{2a}$$

or $$z_1 = z_3 = z_6 = z_7 = 0 \qquad \text{at } y = 0, \text{ for adialatic wall} \tag{2b}$$

$$z_1,\ z_3,\ z_5,\ z_7 \rightarrow 0 \qquad \text{at } y \rightarrow \infty \tag{3}$$

where z's are defined as

$$z_1 = u,\quad z_2 = u_y,\quad z_3 = v,\quad z_4 = p$$
$$z_5 = \theta,\quad z_6 = \theta_y,\quad z_7 = w,\quad z_8 = w_y \tag{4}$$

and a_{mn} is a variable coefficient matrix. Nonzero elements of this matrix are given in reference 2.

Similar suction parameter γ, used to study the effect of suction, is defined as

$$\gamma = \frac{(\rho^* V^*)_w}{(\rho^* U^*)_\infty} R \tag{5}$$

Equations (1), with boundary conditions (2) and (3), are solved using a variable stepsize integrator written by Scott and Watts (ref. 13).

3. RESULTS AND DISCUSSION

Neutral stability curves of 2nd and 3rd mode were studied for Mach numbers from 0 to 4. Contours of constant growth rates were plotted for $m_\infty = 0.0$ and 3.0 for two higher modes to study the growth of these higher eigenstates and to compare the amplitude ratio with that of the fundamental mode. The effect of suction has primarily been discussed for $m_\infty = 3.0$ (see section 3.5).

3.1 Neutral Stability

Figure 1 shows the plot of neutral stability curves ($\alpha = 0$) for the 2nd mode of disturbances for different Mach numbers. Figure 2 shows the same curves for 3rd eigenstates and it is obvious, by comparing the two figures, that the family of curves move upward on the G,B plane for higher modes suggesting stabilizing effect of higher Mach numbers. The value of the Goertler number corresponding to the minimum of the curves is known as critical Goertler number. This number represents the local stability limit. Figure 3 is a plot of critical Goertler number as Mach number for different modes. As the mach number is increased the critical Goertler number is not affected and remains constant until a point where it starts increasing. This is true for 2nd and 3rd mode; however, for the fundamental mode the curve increases continuously with the Mach number. This suggests a delayed stabilizing influence of compressibility on higher modes.

3.2 GROWTH RATES OF HIGHER EIGENSTATES

Figures 4 and 5 show the contours of constant growth rates of 2nd and 3rd mode for $m_\alpha = 0.0$. Figures 6 and 7 show the same contours for $m_\alpha = 3.0$.

As can be inferred from the neutral stability curves (figs. 1 and 2), the family of curves for constant amplification rates move up in the G, β plane for higher eigenstates. This indicates that the fundamental mode may be the most predominant of all existing modes as far as local stability is concerned.

Lines of maximum growth are shown in figures 4 to 7 by dash lines, and it can be thought of as the path along which vortices are most likely to grow since a minimum of the curves corresponds to the most unstable wave number.

3.3 EIGENFUNCTIONS OF HIGHER MODES

Figures 8a to 8d give a comparison of the shape of 2nd eigenstates of disturbance quantities u, v, w and θ, respectively, at different Mach numbers for a wave number of $\beta = 0.6$ and a growth rate of $\alpha = 2$. The corresponding Goertler numbers for $m_\alpha = 0,1,2,3$, and 4 are G = 14.57, 13.757, 12.492, 12.499 and 14.683. The value of u, v, w and θ are normalized with the maximum of u component for the corresponding Mach number.

Figures 9(a-d) give a comparison of the shape of 3rd eigenstates for $m_\alpha = 0,1,2,3$ and 4. The flow conditions are the same as in figures 8(a-d). The corresponding Goertler numbers in this case are G = 31.01, 28.803, 25.195, 23.699, and 25.771. It can be seen from figures 8 and 9 that the location of u_{max}, v_{min} and θ_{max} move away from the wall as the Mach number increases. This shows that the effect of compressibility on higher eigenstates is similar in nature to that of the fundamental mode, and the disturbances persist in a larger region as the Mach number increases.

3.4 AMPLITUDE RATIO OF HIGHER MODES

The critical Goertler number is not a useful quantity if transition prediction is required. Growth of vortices must be taken into account. The

total growth of vortices can be represented in terms of amplitude ratio, which can be defined in terms of G and σ, as follows:

$$\ln \frac{a}{a_o} = \frac{4}{3} \int_{G_o}^{G} \frac{\sigma}{G} dG \tag{6}$$

where a_o and G_o are the amplitude and Goertler number corresponding to the neutral stability.

Integration of equation (6) can be done along various paths. Figure 10 shows the plot of amplitude ratio vs. Goertler number G for the first three eigenstates for $m_\alpha = 0.0$. It can be seen from this figure that 2nd and 3rd mode not only originate after 1st mode but also the rate of growth of amplitude (slope of curves) decreases for higher modes. This indicates again that the fundamental mode is the dominant mode at $m_\alpha = 0.0$.

Figure 11 shows the same curve for $m_\alpha = 3.0$, and all previous observations regarding figure 10 apply to it. In the above analysis the integration was done along the maximum growth path until $G = 45$. Experimentally the wavelength of the vortices have been found to be conserved along the length of curved surface (ref. 12). Lines of constant wavelengths can be shown to have tangent 3/2 on the G.B. plane and are defined by the nondimensional parameter Λ, as follows:

$$\Lambda = \frac{U_\infty \lambda}{\nu_\infty} \left(\frac{\lambda}{r}\right)^{1/2} \tag{7}$$

This can be written in terms of G and β as

$$\Lambda = \frac{G}{\beta^{3/2}} \tag{8}$$

Amplitude ratios are calculated for constant Λ for different eigenstates by integrating equation (6) until $G = 45$ for $m_\alpha = 3.0$. The result is shown in figure 12.

It is interesting to observe that the most unstable wavelength corresponding to the peak of the curves is the same for 2nd and 3rd mode, and is approximately equal to 40. The same quantitative observation was made by Herbert (ref. 5) for incompressible fluids. Large reduction in amplitude ratio is observed for higher modes. It can also be seen that the cut-off wavelength increases for higher modes.

3.5 EFFECT OF SUCTION ON HIGHER EIGENSTATES

Figure 13 shows the neutral stability curves for different values of suction parameter ν, for 2nd and 3rd mode, for $m_\infty = 3.0$. The critical Goertler number increases with suction in both higher modes. This can be seen more clearly in figure 14. However, for the fundamental mode the critical Goertler number first decreases and then increases as suction is increased.

The overall effect of suction on the fundamental mode and higher modes still remains stabilizing, as can be seen from figure 11, where amplitude ratio has been plotted against G for $m_\infty = 3.0$ and $\nu = -1.2$.

Figures 15(a-d) and 16(a-d) show the shape of eigenfunctions for three different values of ν for 2nd and 3rd mode, respectively. It is clear from these figures that the effect of suction is in bringing the disturbances closer to the wall where viscous dissipation is higher and, thereby, stabilizing the flow.

4. CONCLUSIONS

Fundamental eigenstate of Goertler instability seems to dominate the flow, and higher eigenstates play a smaller role in controlling the growth of vortices of the different eigenstates, which are assumed to exist independently.

Obviously, the actual phenomenon of Goertler instability is nonlinear and would require an understanding of the interaction between different modes. However, the present linear theory does give us an insight into the problem.

The "most dangerous" wavelength for fundamental and higher modes is nearly the same.

Suction seems to have a locally stabilizing influence on higher modes contrary to the initial destabilizing influence observed on the fundamental mode.

The overall effect of suction on higher modes is stabilizing.

REFERENCES

1. Goertler, H.: On the Three-Dimensional Instability of Laminar Boundary Layers on Concave Walls. NASA Tech. Memo. 1357, 1954. (Translation of "Uber Eine Dreidimensionale Instabilitat Laminarer Grenzschichten an Konkaven Wanden," Ges. d. Wiss. Gottinten, Nachr, a.d. Math., Bd. 2, Nr. 1, 1940.)

2. El-Hady, N.M. and Verma, A.K.: Goertler instability in compressible boundary layers along curved surfaces with suction and cooling. NASA CR-3544, 1982.

3. Lin, G.C.: The theory of hydrodynamic stability. Cambridge University Press, 1955.

4. Aihara, Y.: Nonlinear Analysis of Goertler Vortices. Phys. Fluids 19 1976, pp. 1655-1660.

5. Herbert, T.: Higher eigenstates of Goertler vortices. Development in theoretical and experimental fluid mechanics. Edited by Muller and Rosener.

6. Aihara, Y.; and Sonoda, T.: Effects of Pressure gradient on the secondary instability of Goertler vortices. AIAA-81-0197, St. Louis, Missouri, 1981.

7. Wortmann, F.X.: Visualization of Transition. J. Fluid Mech. 38, 1969, pp. 473-480.

8. Bippes, H: Experimental Study of the Laminar-Turbulent Transition of a Concave Wall in a Parallel Flow. NASA TM-75243, 1978. (Translation of "Experimentelle Untersuchung Laminar-Tuirbulenten Umschlags an Einer Parallel Angestromten Konkaven Wand," Heidelberger Akademie der Wissenschften, Mathematisch-Naturwissenschftlichg Klasse, Sitzungsberichte, No. 3, 103-180, 1972).

9. Aihara, Y.; Goertler vortices in the nonlinear region. Development in theoretical and experimental fluid mechanics. Edited by Muller and Rosener.

10. El-Hady, N.M., and Verma, A.K.: Growth of Goertler Vortices in Compressible Boundary Layers Along Curved Surfaces. AIAA Paper No. 81-1278, 1981. Presented at the 14th Fluid and Plasma Dynamic Conference, Palo Alto, CA, June 23-25,

11. El-Hady, N.M.; and Verma, A.K: Instability of compressible boundary layers along curved walls with suction or cooling. AIAA Paper No. 82-1010, 1982. Presented at the 3rd AIAA/ASME Joint Thermophysics, Fluids, Plasma and Heat Transfer Conference, St. Louis, MO, June 7-11, 1982.

12. Beckwith, I.E.; and Holley, B.B.: Goertler vortices and transition in the wall boundary layers of two Mach 5 nozzles. NASA TP no. 4546, 1980.

13. Scott, R.R.; and Watts, H.A.: Computational solution of linear two point boundary-value problems via orthonormalization. SIAM J. Num. Anal, 14, 1977, pp. 40-70.

ORIGINAL PAGE IS
OF POOR QUALITY

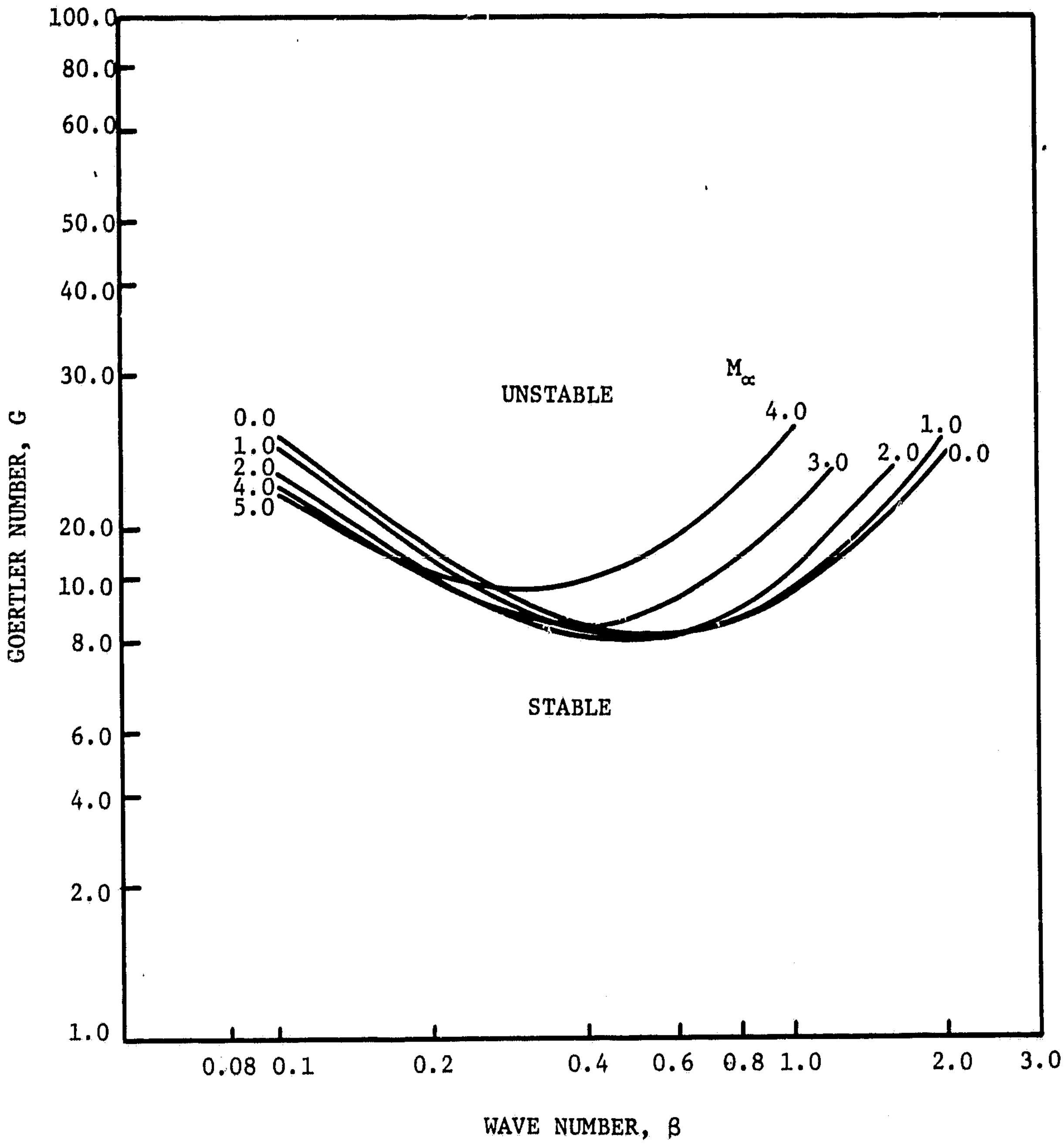

Figure 1. Neutral stability curves of 2nd mode for different Mach numbers.

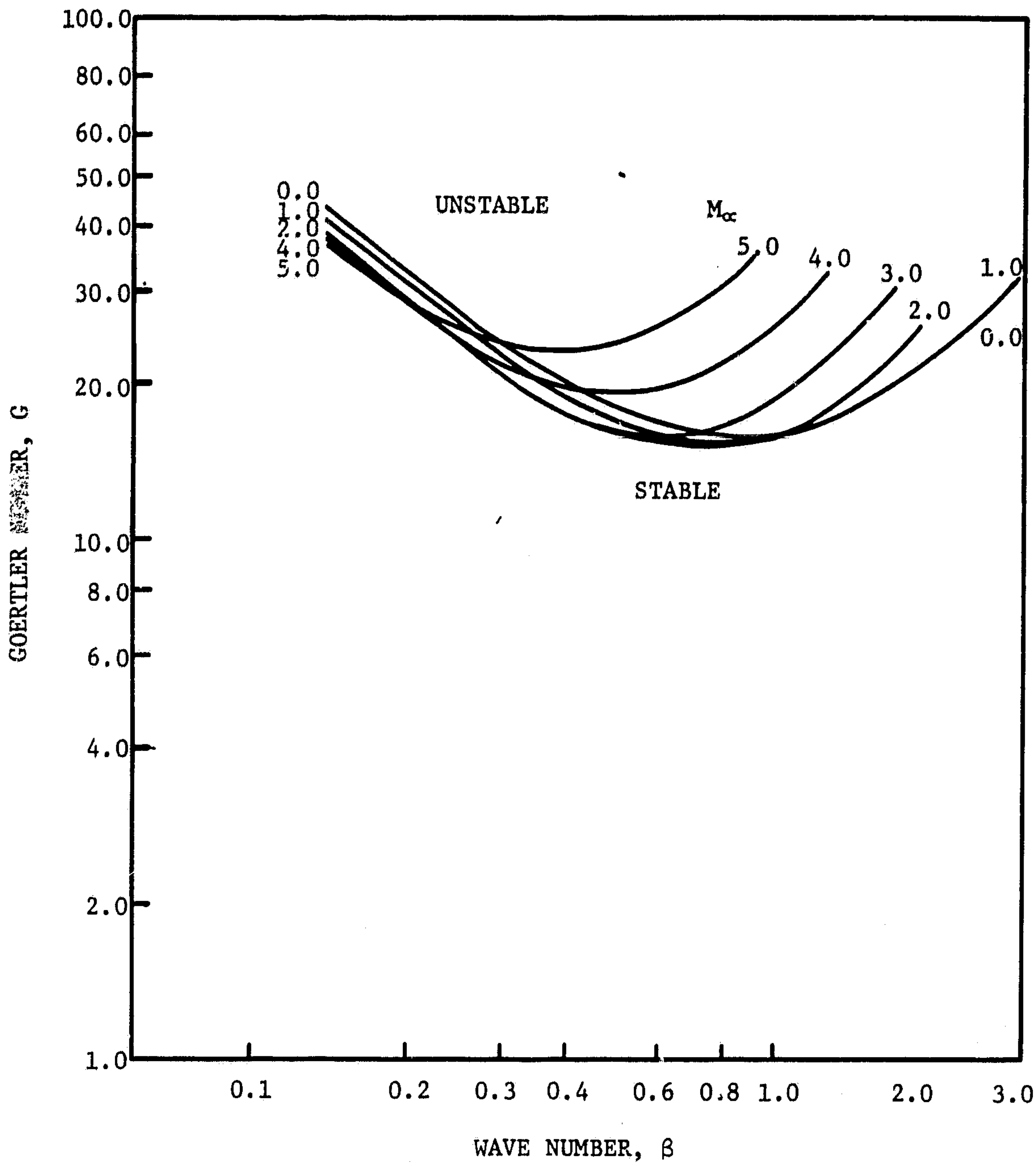

Figure 2. Neutral stability curves of 3rd mode for M_∞ = 1 - 5.

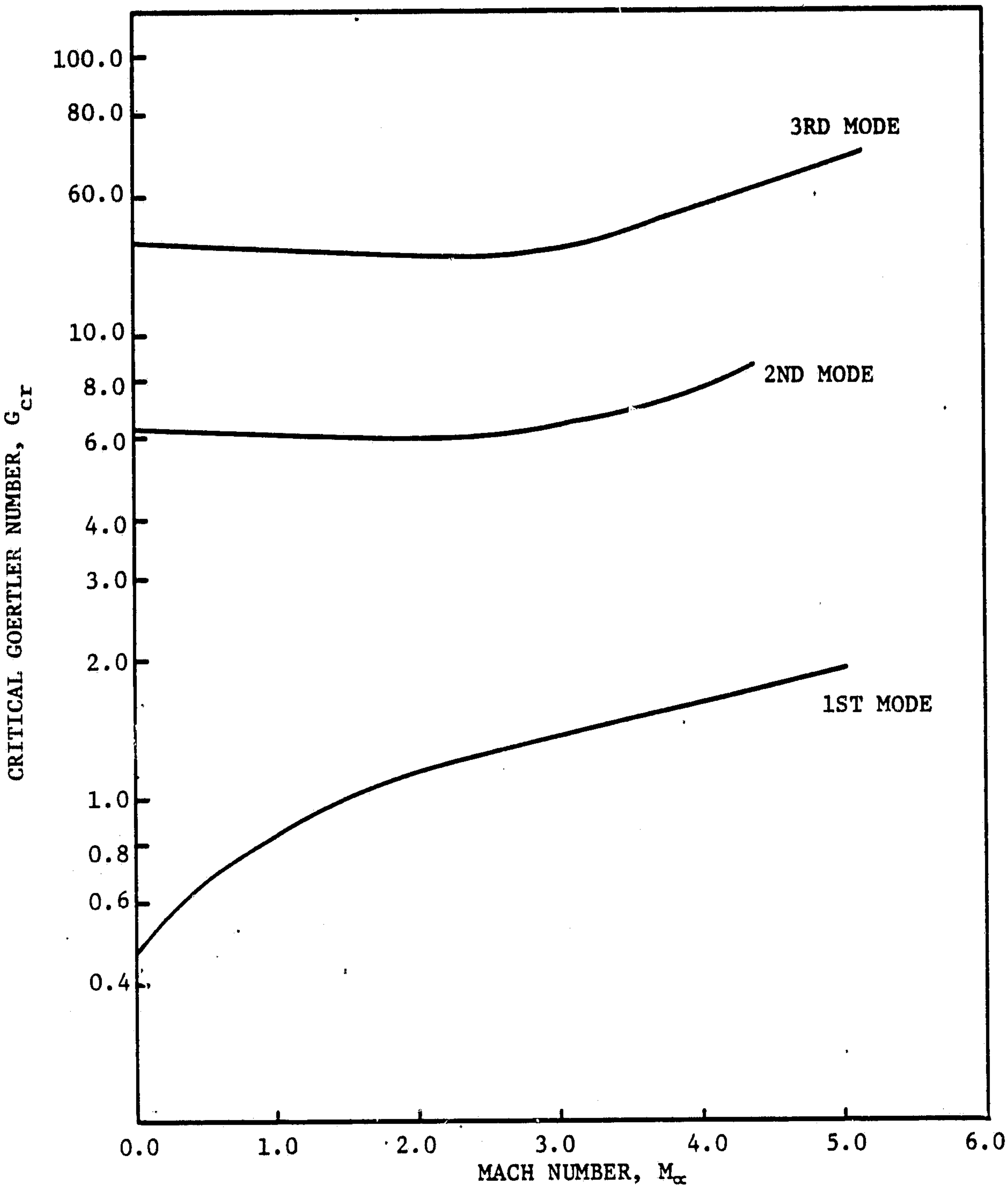

Figure 3. Effect of compressibility on local stability of higher modes.

ORIGINAL PAGE IS
OF POOR QUALITY

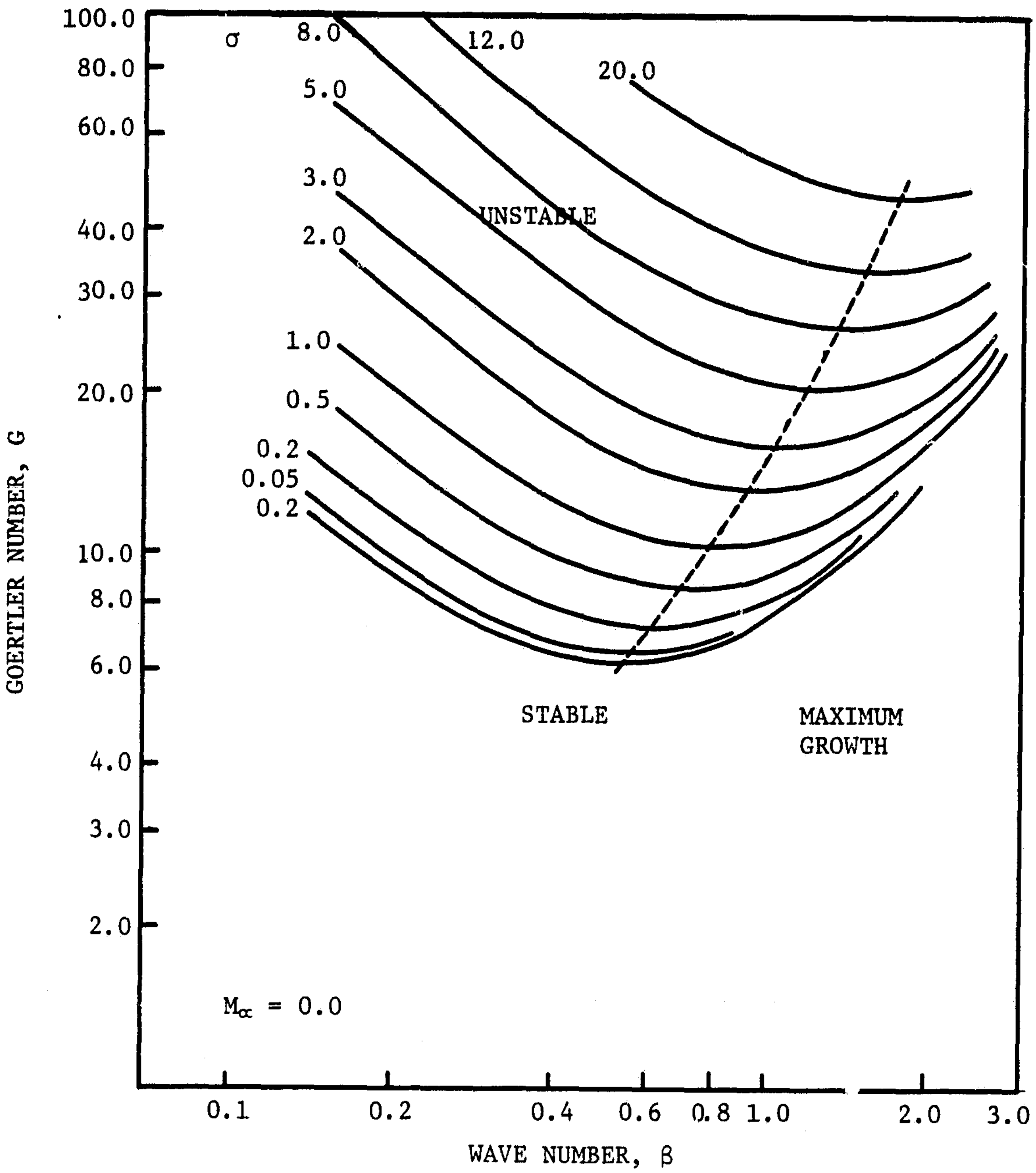

Figure 4. Contours of constant growth rates of 2nd mode for $M_\infty = 0.0$.

ORIGINAL PAGE IS
OF POOR QUALITY

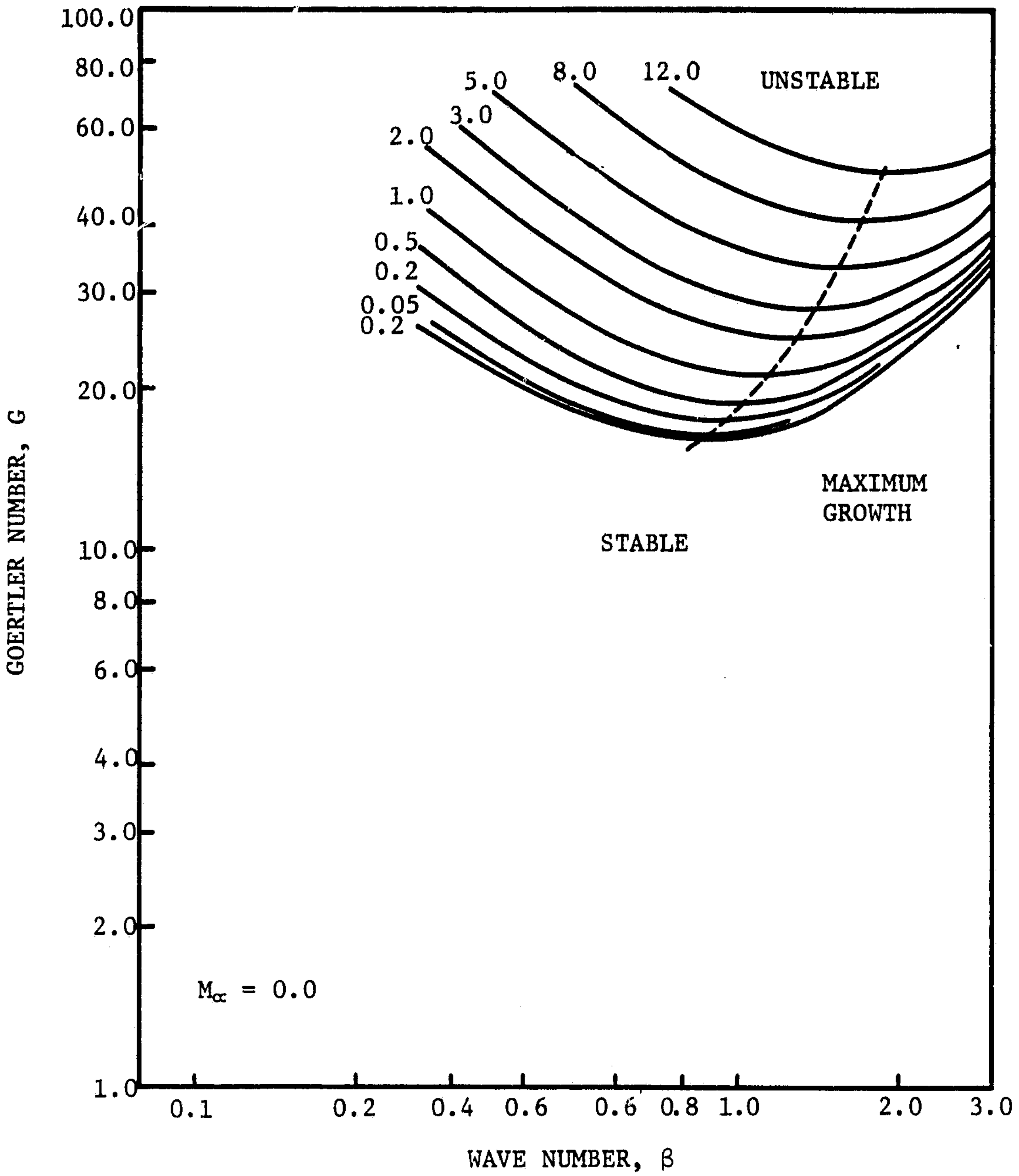

Figure 5. Contours of constant growth rates of 3rd mode at M_∞ = 0.0.

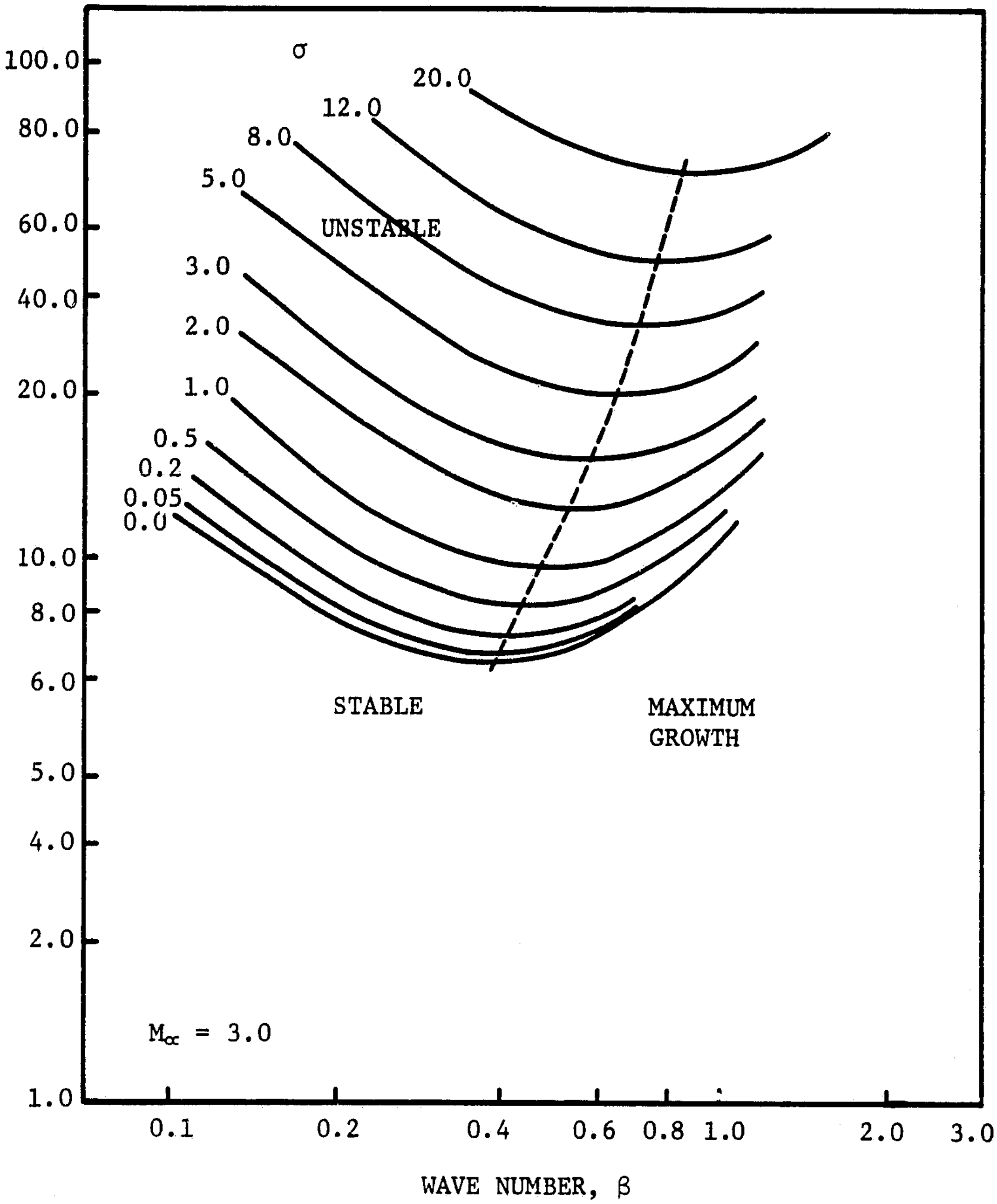

Figure 6. Contours of constant growth rates of 2nd mode at $M_\infty = 3.0$.

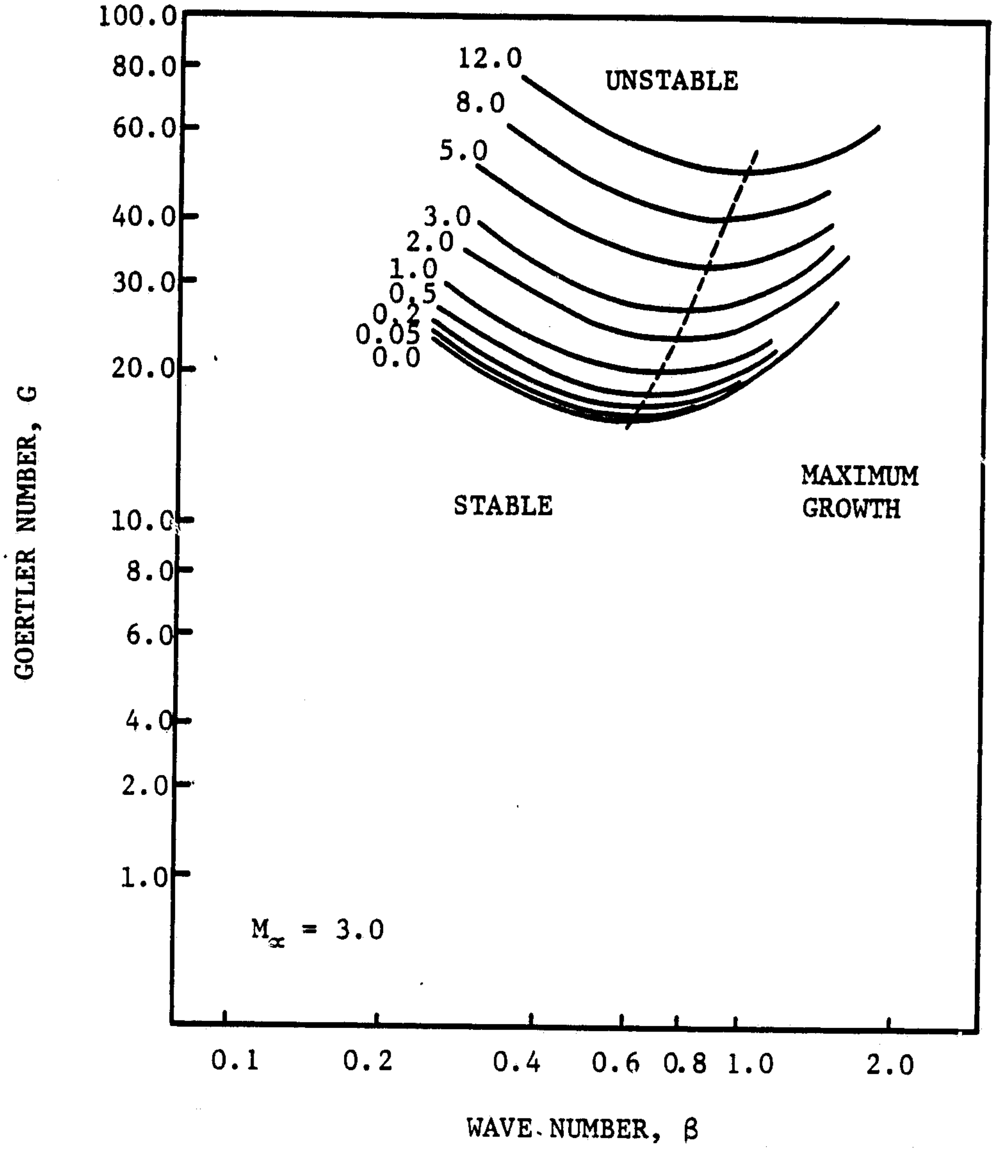

Figure 7. Contours of constant growth rates of 3rd mode at $M_\infty = 3.0$.

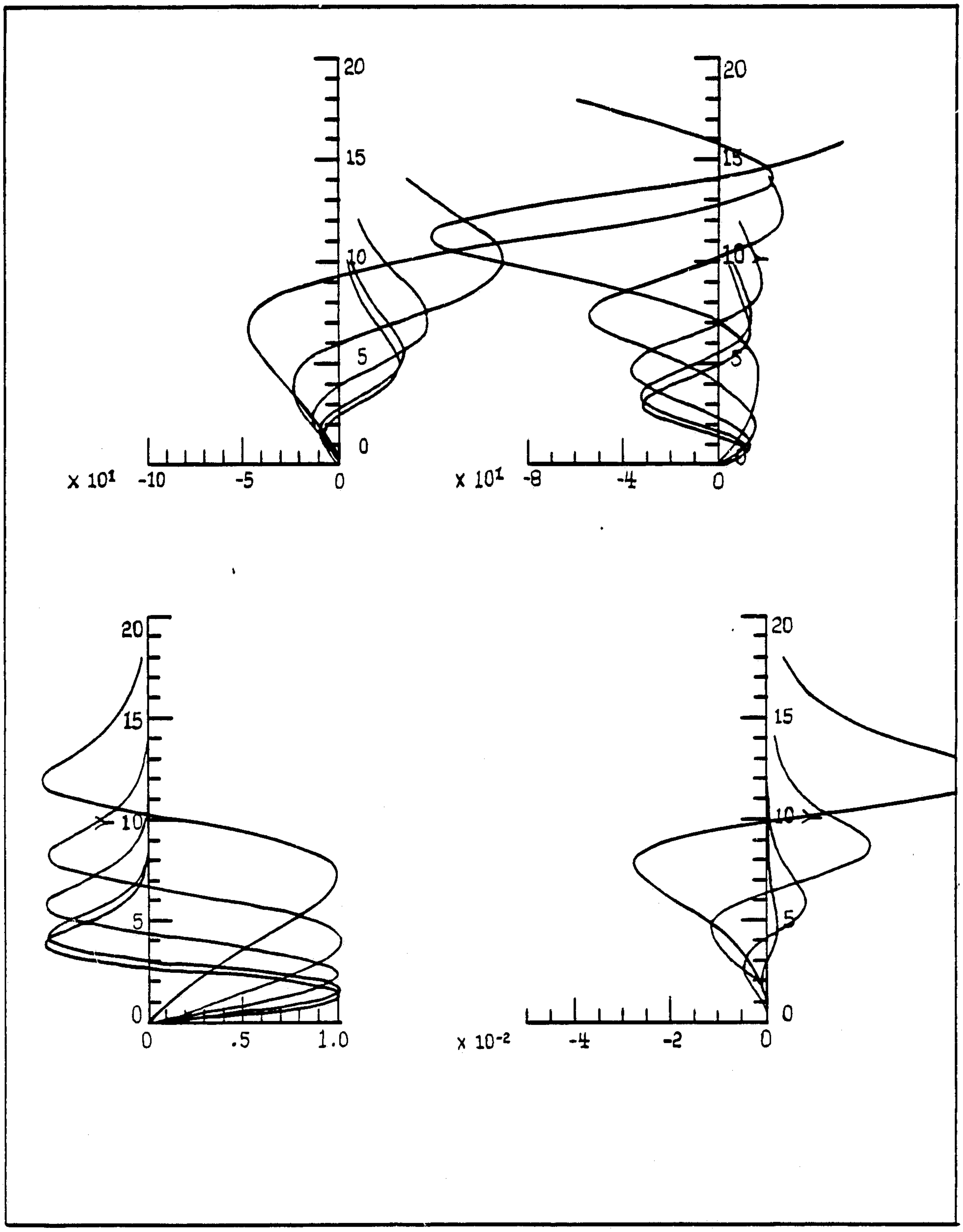

Figure 8. Shape of eigenfunctions of 2nd mode for $M_\infty = 0 - 4$.

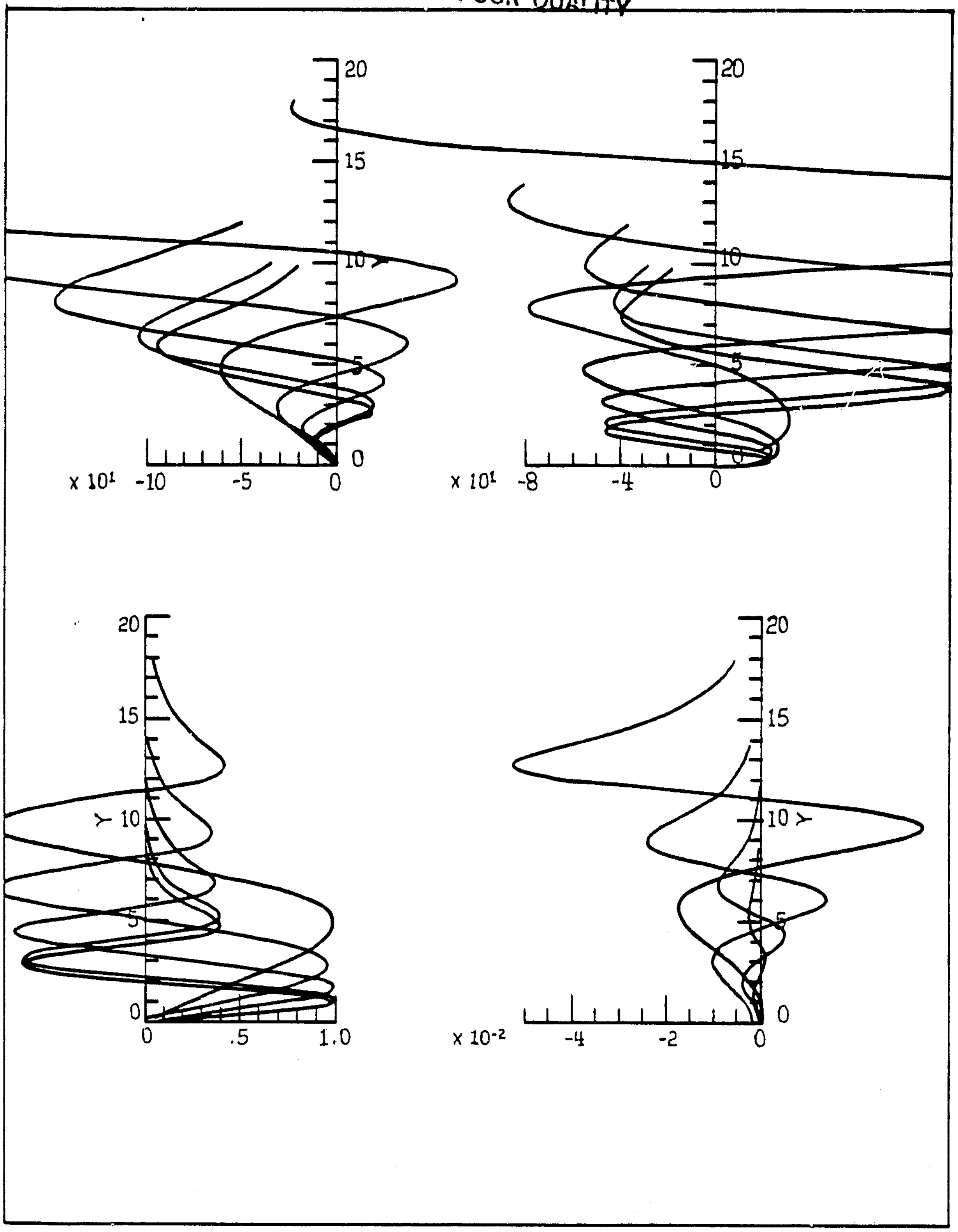

Figure 9. Shape of eigenfunctions of 3rd mode for $M_\infty = 0 - 4$.

ORIGINAL PAGE IS
OF POOR QUALITY

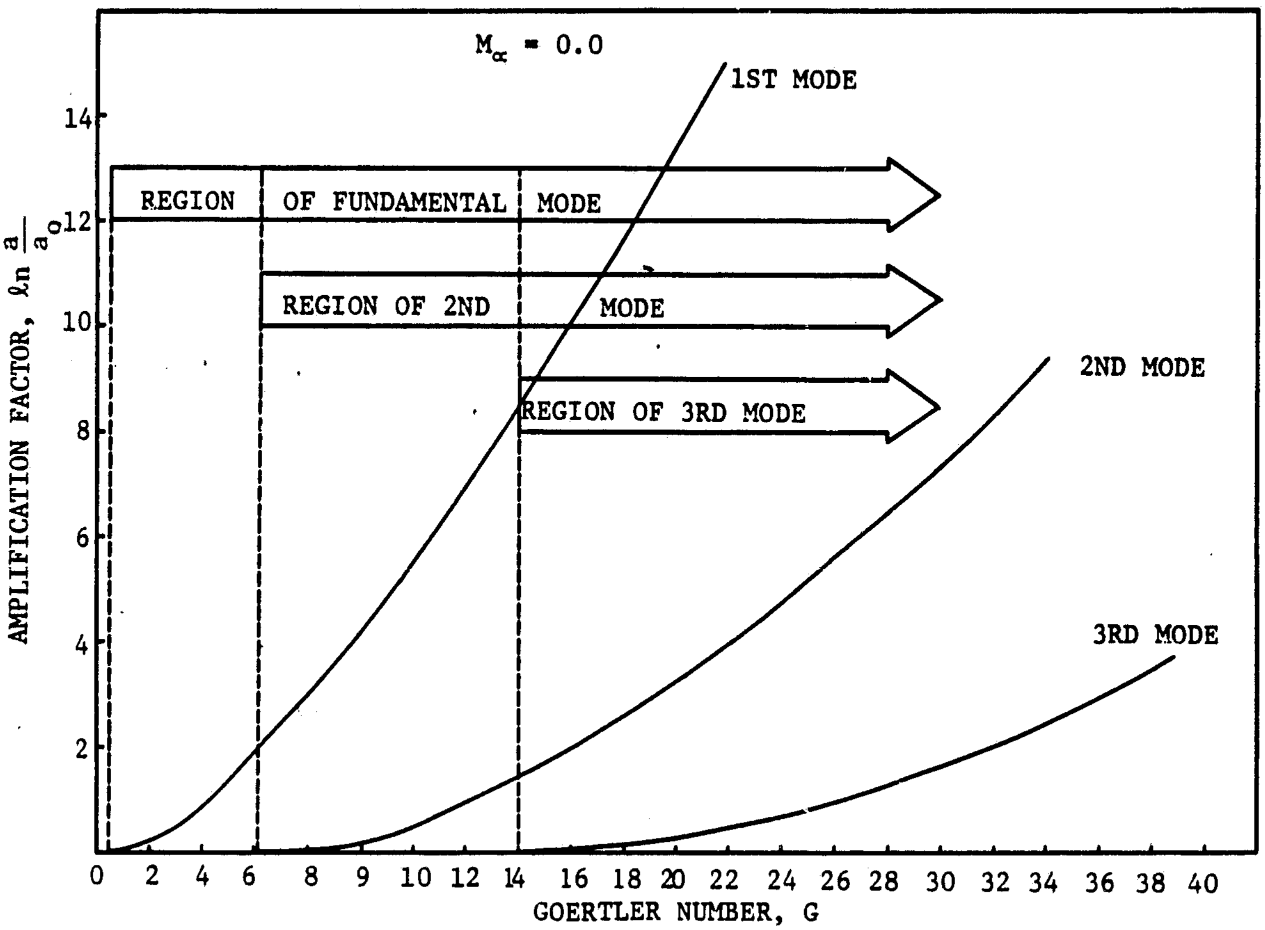

Figure 10. Effect of higher modes on amplitude ratio calculated along the locus of maximum growth rates at $M_\infty = 0.0$.

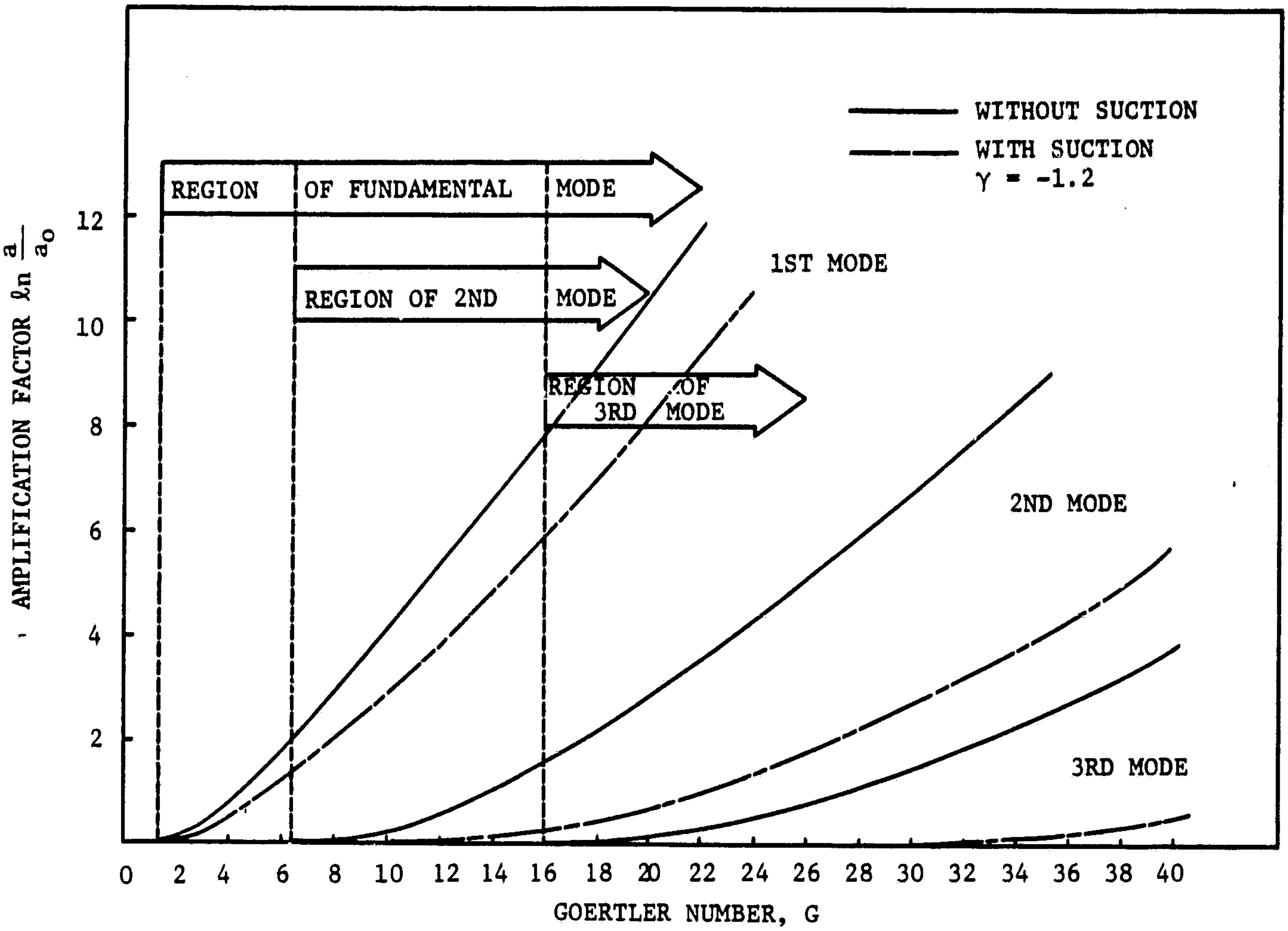

Figure 11. Effect of higher modes on amplitude ratio calculated along the locus of maximum growth rates at $M_\infty = 3.0$. Effect of suction ($\gamma = -1.2$) on these modes.

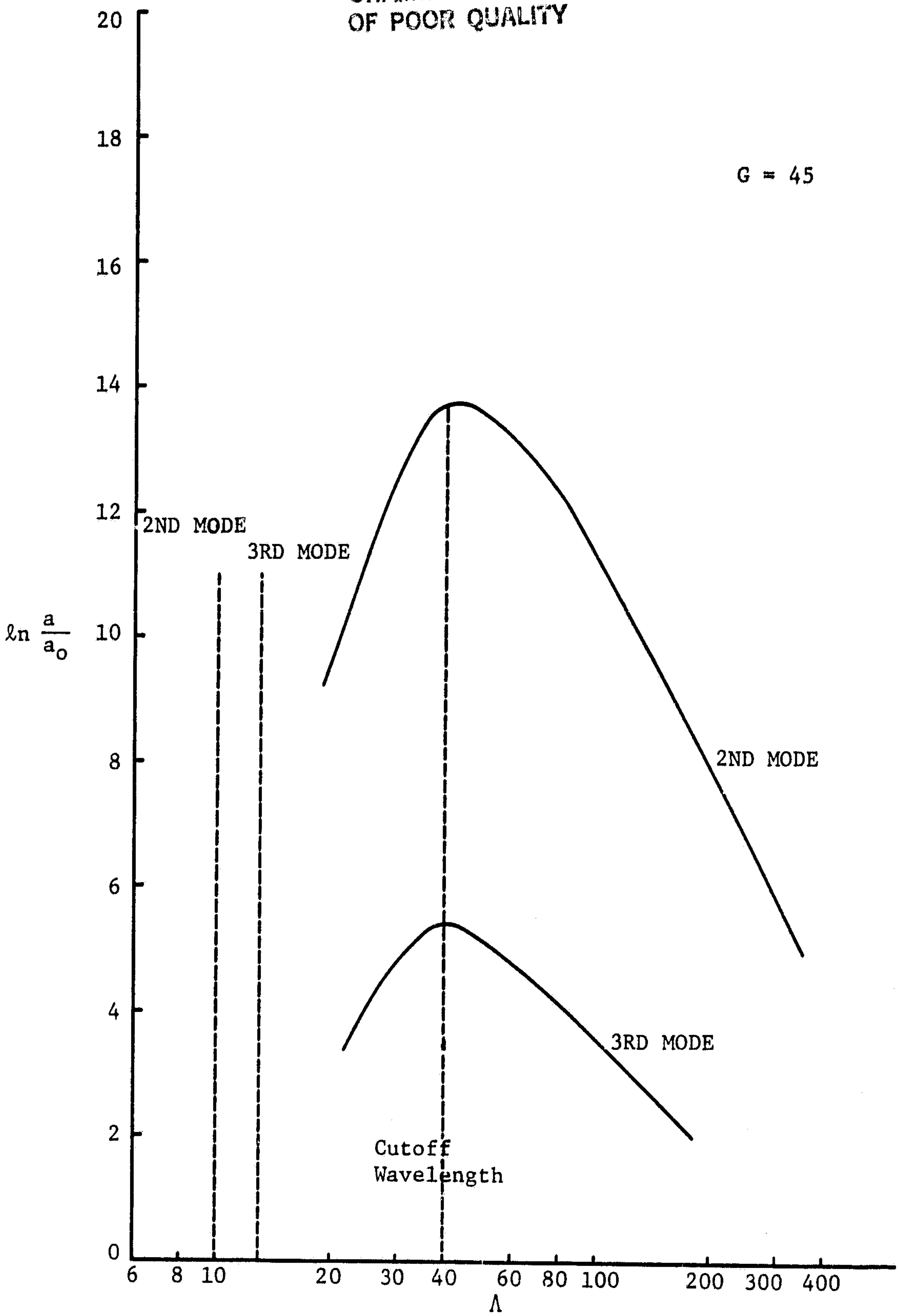

Figure 12. Effect of higher eigenstates on the maximum amplitude ratio calculated along a growth bath of constant wavelength λ.

ORIGINAL PAGE IS
OF POOR QUALITY

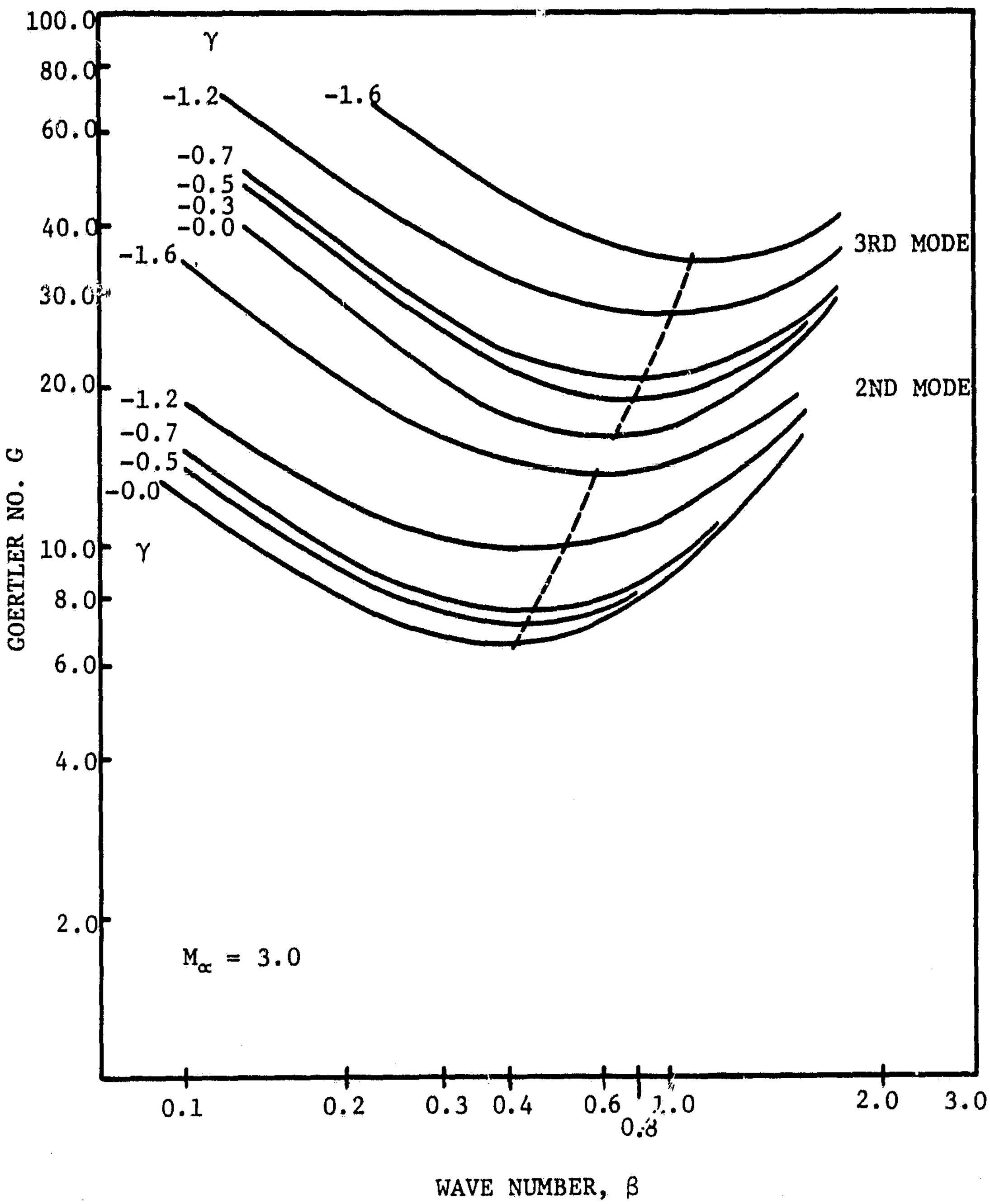

Figure 13. Effect of suction on neutral stability curves for 2nd and 3rd mode for $M_\infty = 3.0$.

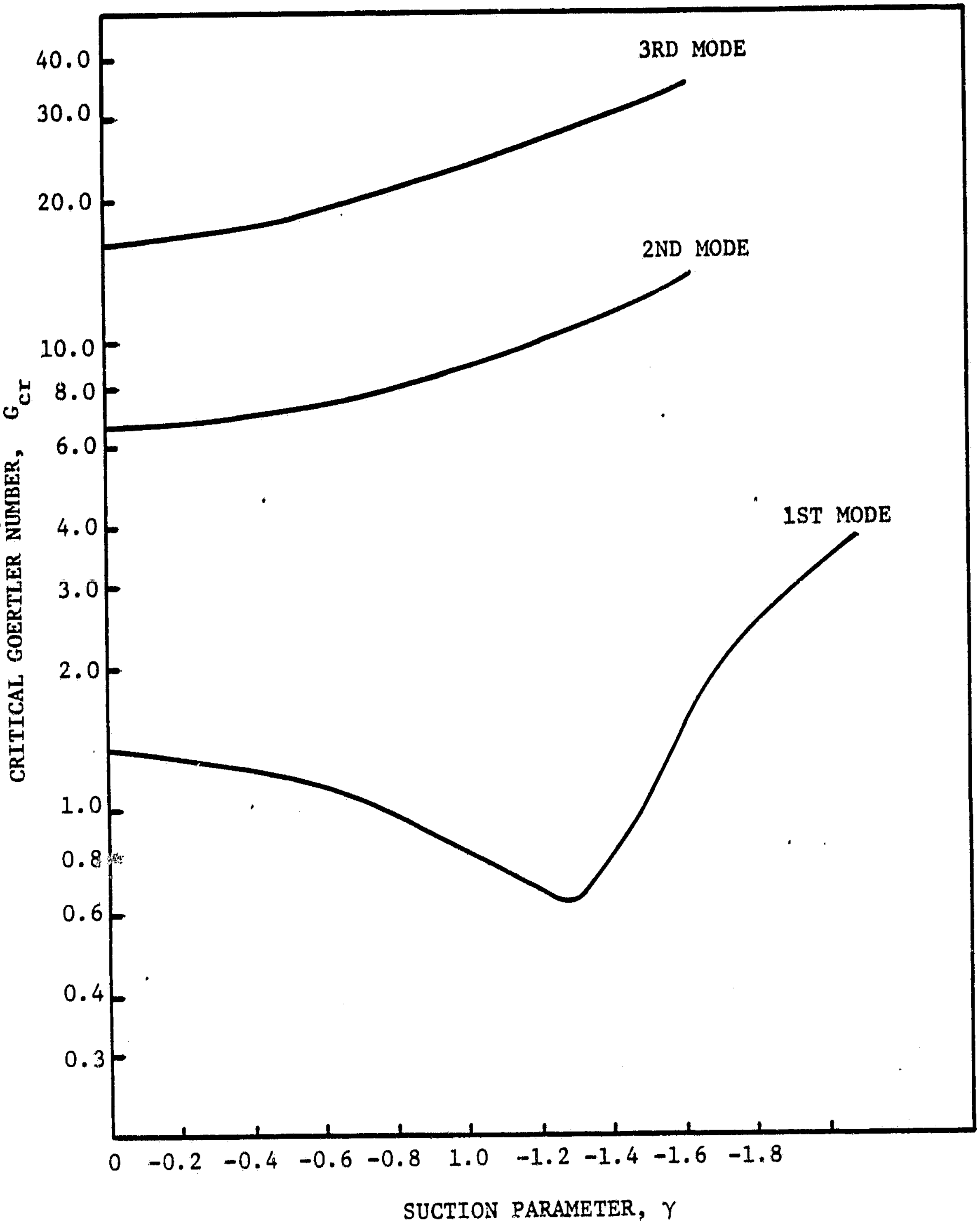

Figure 14. Effect of suction on local stability of higher modes.

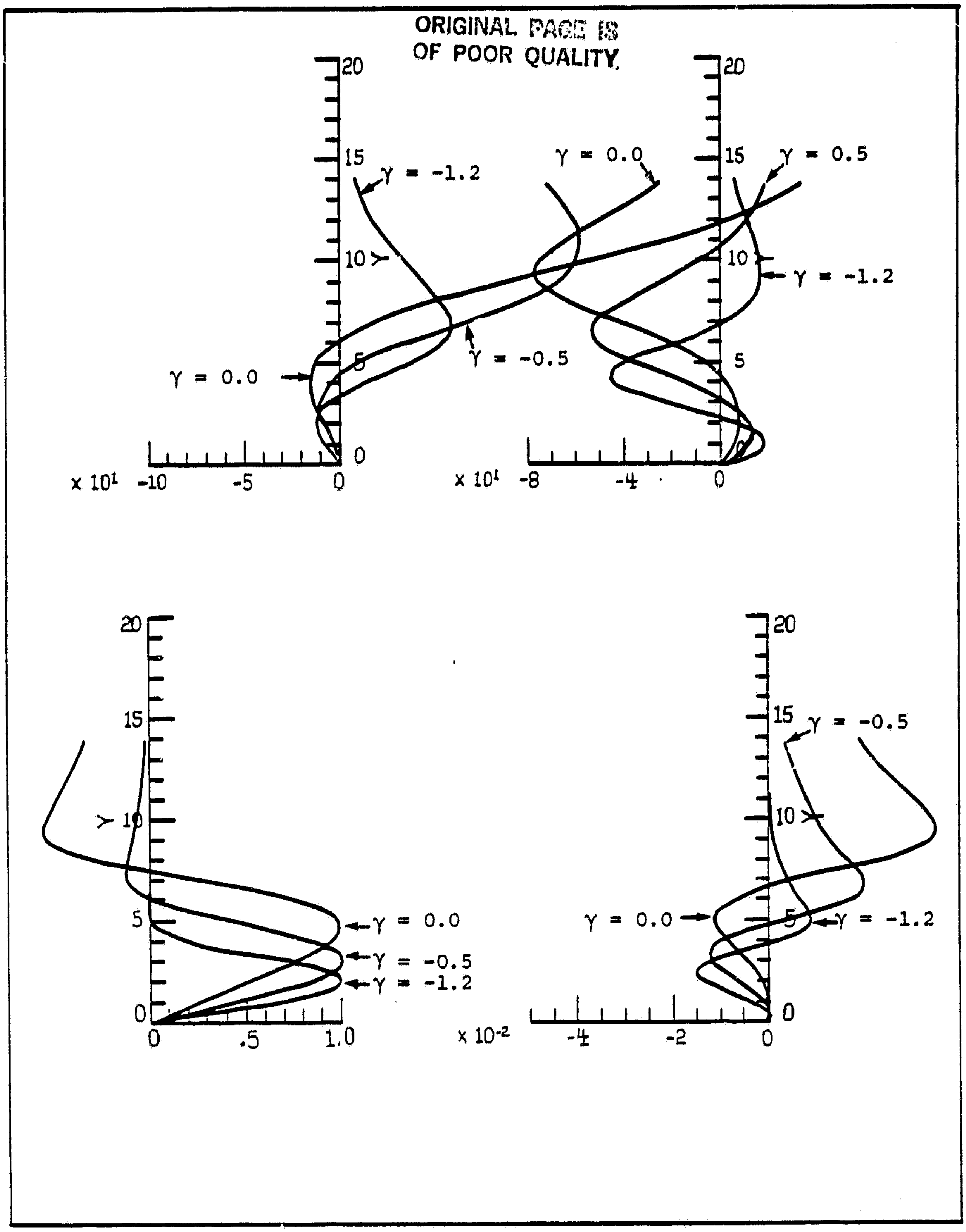

Figure 15. Shape of eigenfunctions of 2nd mode at $M_\infty = 3.0$ for $\gamma = 0.0$, -0.5 and -1.2.

ORIGINAL PAGE IS
OF POOR QUALITY

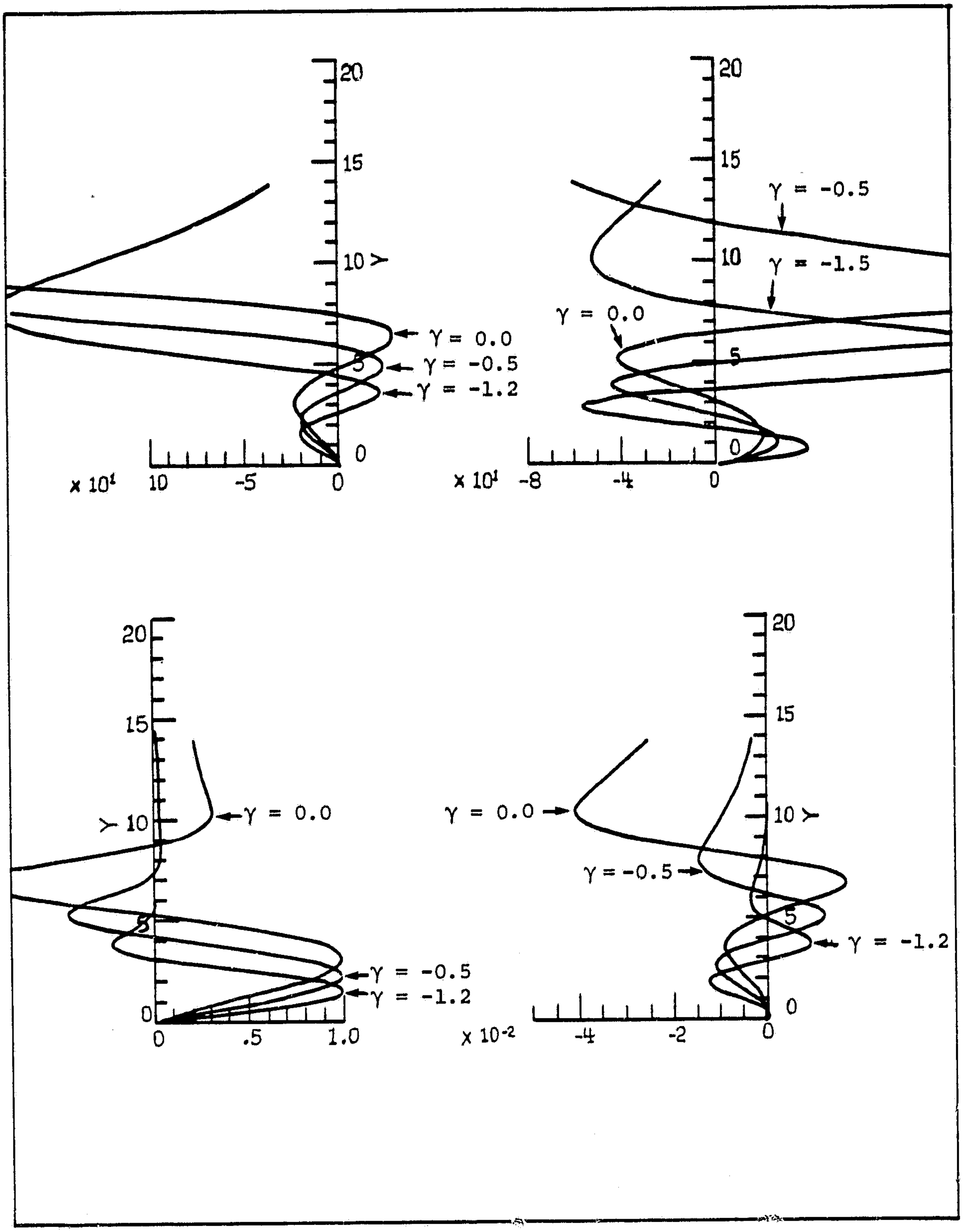

Figure 16. Shape of eigenfunctions of 3rd mode at $M_\infty = 3.0$ for $\gamma = 0.0$, -0.5 and -1.2.